INTERNATIONAL JOURNAL OF ENERGY STUDIES

e-ISSN: 2717-7513 (ONLINE); homepage: https://dergipark.org.tr/en/pub/ijes

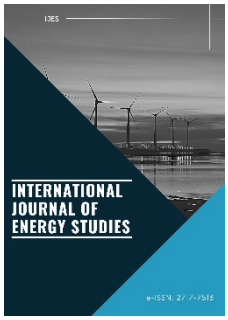

Research Article
Int J Energy Studies 2024; 9(3): 399-422
DOI: 10.58559/ijes.1507464

Received : 30 June 2024
Revised : 13 July 2024
Accepted : 24 July 2024

The impact of turbulence models and design parameters on solar chimney power plant efficiency: A CFD study

Fuat Tan[a*], Alp Eren Dede[b]

[a]*Department of Mechanical Engineering, Faculty of Engineering, Balikesir University, Balıkesir, 10145, Türkiye, ORCID: 0000-0002-4194-5591*

[b]*Department of Mechanical Engineering, Faculty of Engineering, Balikesir University, Balıkesir, 10145, Türkiye, ORCID: 0009-0009-5391-8695*

*(*Corresponding Author: fuattan@balikesir.edu.tr)*

Highlights

- The effects of SCPP chimney height, chimney radius and collector height on performance have been numerically investigated.
- The impacts of RNG k-ε and SST k-ω turbulence models on velocity, temperature and pressure distribution have been simulated.
- The velocities and temperatures influenced by the design parameters and turbulence model are compared in the form of graphs.

You can cite this article as: Tan F, Dede AE. The impact of turbulence models and design parameters on solar chimney power plant efficiency: A CFD study. Int J Energy Studies 2024; 9(3): 399-422.

ABSTRACT

This study numerically examines the effects of chimney height, chimney radius and collector height on the velocity, pressure and temperature distribution in a Solar Chimney Power Plant (SCPP). The analyses were performed using ANSYS Fluent software with two different turbulence models (RNG k-ε and SST k-ω). The results show that increasing the chimney height significantly boosts the outlet velocity but decreases the outlet temperature. Conversely, as the chimney radius increases, the outlet velocity decreases and the outlet temperature slightly drops. Changes in collector height result in complex behavior for both turbulence models in terms of outlet velocity and temperature, highlighting the importance of an optimal collector height. The study includes detailed and numerical data on how different turbulence models can be used for performance analysis and optimization. According to the analysis results, increasing the chimney height from 100 meters to 200 meters resulted in a 35% increase in outlet velocity and a 20% decrease in outlet temperature in the RNG k-ε model. In the SST k-ω model, the same increase raised the outlet velocity by 30% and decreased the outlet temperature by 15%. The research showed that both RNG k-ε and SST k-ω turbulence models respond notably to changes in collector height and design parameters. The RNG k-ε model reacts more quickly and sensitively, while the SST k-ω model behaves more steadily.

Keywords: SCPP, Efficiency, CFD, Turbulence model, Design

1. INTRODUCTION

In recent years, population growth and living conditions worldwide have significantly impacted water and energy demand [1]. The lives of people, particularly those in isolated regions lacking supply networks, are at risk due to the energy crisis and the scarcity of clean, fresh water. Approximately 785 million people globally lack access to clean freshwater and every day, 800 children face health issues due to the scarcity and poor quality of freshwater [2]. This situation leads to the death of a child every two minutes in countries such as Mozambique, Ethiopia and Liberia. Although water covers 75% of the Earth's surface, only a small fraction of freshwater resources is usable by humans [3]. Fossil fuels are the primary energy sources for electricity generation and water desalination, still accounting for approximately 80% of global energy consumption [4]. Although these fuels produce a significant amount of electricity, they also pollute water and air. [5,6]. In particular, CO2 emissions, a greenhouse gas, can lead to climate change and the global warming crisis. Consequently, many countries worldwide are exploring renewable energy technologies and seeking to replace traditional energy sources with alternative ones.

Currently, the most widely used renewable energy sources include solar, wind, tidal, hydroelectric, geothermal and biomass energy [7]. One of the most promising sources is solar energy, which is very clean and abundant compared to other sources. The Solar Chimney Power Plant (SCPP) exemplifies a renewable energy technology that can help decrease reliance on conventional energy sources [8]. SCPPs, based on solar thermal energy, have garnered significant interest for electricity generation. This system is a long-lasting, environmentally friendly technology that does not require water cooling.

Since the air collector can absorb both direct and diffuse radiation, its performance is not dependent on weather conditions. Additionally, this system can be constructed easily and simply with inexpensive materials. The soil placed beneath the system can be used as a storage medium for future benefits [9]. This system consists of a chimney, an air collector, a turbine and a generator [10]. The production of freshwater and electricity using traditional technologies requires high costs and demands more energy. Therefore, many studies aim to integrate renewable energy technologies, which are environmentally sustainable methods, with desalination and electricity generation systems. Tawalbeh et al. [11] investigate a configuration based on hybrid solar chimney technology, capable of producing both water and electricity, which maximizes the use of advanced transparent photovoltaics and desalination to enhance system efficiency and power generation.

A solar plant was constructed in Manzanares, Spain and the data obtained from this solar plant were analysed by Haaf [12]. To date, a full-scale solar chimney power plant has not been constructed; however, a 200 MW solar tower project is currently under development in Australia. The cost of energy generated by a solar chimney varies significantly based on location, labor costs and material costs, highlighting the need for further research. Reports indicate that a SCPP in the Mediterranean region generates significantly more electricity compared to other energy sources. [13]. Zhou et al. [14] indicated that both the maximum height for convection and the optimal height for maximum power output increase as the collector radius becomes larger. Many researchers presume that the overall efficiency of the power conversion unit is 80%, which has been examined by different scientists. It was also observed that the efficiency of the power conversion unit decreases significantly with a larger diffuser area ratio, while it shows only a slight increase when the ratio is less than one [15].

Conversely, it has been asserted that large-scale systems can achieve output power up to 1000 MW. Following the successful establishment of conservation equations for solar chimney power plants, performance feasibility studies for systems likely to be installed in different climate regions have been conducted [16]. A numerical study by Maia et al. [17] aligned well with earlier experimental research and highlighted that the tower's height and diameter are the most crucial physical factors in SCPP design. The effects of geometric parameters, particularly chimney height and collector radius, on system performance have been numerically studied by many researchers [18]. A numerical optimization study has shown that increasing the collector slope enhances the mass flow rate of air movement within the system, improving the system's power output [19]. According to the study by Cuce et.al. [20], solar chimney power plants can achieve maximum power output with a 0.6° collector slope and a 1.5° chimney divergence angle. Additionally, the use of an Artificial Neural Network (ANN) model with 9 neurons has shown high accuracy in predicting SCPP system performance. According to the study by Mandal et al. [21], the optimal combination of a ground sloped absorber and a divergent chimney can increase power generation by up to 80% (92 kW) compared to the classical Manzanares plant.

In another study by Biswas et al. [22], the potential of SCPPs as sustainable energy sources is highlighted, emphasizing their low cost and eco-friendliness. The study underscores the need for further practical and experimental investigations to bridge the gap between numerical research and real-world applications, aiming to facilitate the commercialization of both standalone and hybrid

SCPPs. In another study [23], the use of a stair-shaped ground surface in chimney-based solar thermal power plants (SCPPs) is investigated, showing that this design can enhance power generation by up to 80%. The analysis, validated against the Manzanares pilot plant, demonstrates that the stair-shaped absorber improves overall plant efficiency and could be a viable alternative for increasing power output in classical SCPPs. In a study by Mandal et al. [24], a modification of the absorber surface with multiple triangular wavy peaks at different amplitudes significantly improves the performance of solar chimney power plants (SCPP). This innovative design enhances power generation by up to 82.5 kW and boosts efficiency by 61.83%, suggesting a promising approach for establishing SCPPs in hilly or wavy terrain to supply power to remote areas.

In another study [25], strategic modifications to the collector inlet height, chimney diameter and chimney divergence in a conventional Manzanares solar chimney plant were examined to optimize power generation. The study found that reducing the collector inlet height and optimizing chimney dimensions could significantly enhance power output, with the best configuration achieving a substantial 12.45-fold increase in power generation, reaching 635.02 kW. In a study by Navarro et al. [26], a detailed transient experimental and numerical analysis of heat transfer and airflow in a scaled room linked with a double-duct vertical roof solar chimney was conducted. The study demonstrated that the transient heating of the solar chimney significantly impacts temperature fields and flow patterns, with correlations provided for Nusselt number and air changes per hour as a function of the modified Rayleigh number. In another study, Maia and Silva [27] analyzed the performance of small-scale solar chimneys exposed to ambient crosswinds. By using ANSYS Fluent for CFD simulations, they demonstrated that increased wind speeds enhanced heat transfer and airflow velocity, which improved the overall efficiency of the solar chimney.

Solar chimneys are typically designed to operate in areas with high levels of direct sunlight and low humidity. Because the heat absorbed by the collector area can be stored in the surrounding materials and gradually released over time, they can generate electricity even without sunlight. The collector area is made of a dark, heat-absorbing material that warms the air inside. As the air heats up, it rises through the chimney, driving a turbine that generates electricity. The height of the chimney creates a pressure difference that helps draw air from the collector area into the chimney. While solar chimneys have the potential to produce significant amounts of electricity, they are relatively expensive to build and require large amounts of land. As a result, they are not

as widespread as other types of renewable energy technologies, such as solar panels or wind turbines.

The aim of this study is to assess the impacts of the RNG k-ε and SST k-ω turbulence models on the thermal and fluid flow characteristics of the solar chimney. To observe the effects of turbulence, the aerodynamic results obtained by varying the design parameter values of chimney height, chimney radius and collector height in the SCPP system were compared with each other.

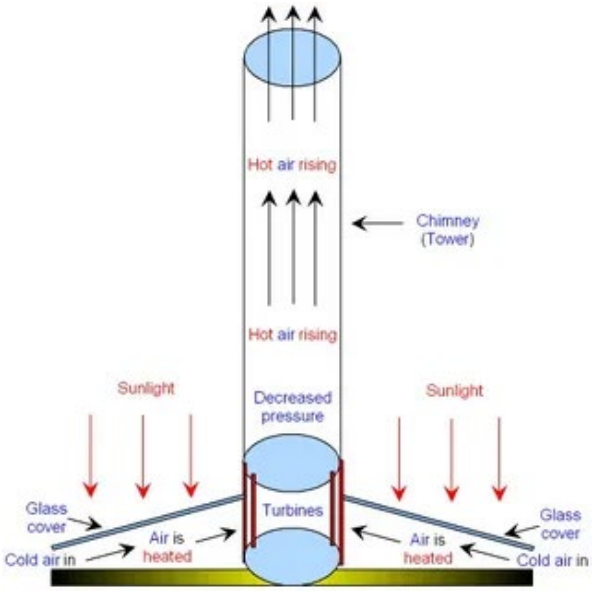

Figure 1. Solar chimney power plant

2. THEORETICAL MATHEMATICAL MODEL [20, 28]

CFD analysis involves several steps, including geometry modeling, meshing, defining boundary conditions, selecting numerical methods and algorithms, solving the equations and post-processing the results. The precision of the results relies on multiple factors, including the quality of the model geometry, mesh quality, accuracy of boundary conditions and the selection of suitable numerical methods. CFD is founded on the Navier-Stokes equations, which are derived from the principles of conservation of mass, momentum and energy. These equations describe how a fluid's velocity, pressure and density change over time in response to external forces and internal friction. The selection of energy equations should take into account the boundary conditions. In this study, the Navier-Stokes and continuity equations were utilized to describe the flow in the x, y and z directions. The momentum equation along the X-axis;

$$\frac{\partial}{\partial t}(\rho u)+\frac{\partial}{\partial x}(\rho uu)+\frac{\partial}{\partial y}(\rho vu)+\frac{\partial}{\partial z}(\rho wu)=-\frac{\partial P}{\partial x}+\mu\left(\frac{\partial^2 u}{\partial x^2}+\frac{\partial^2 u}{\partial y^2}+\frac{\partial^2 u}{\partial z^2}\right) \quad (1)$$

The momentum equation along the Y-axis;

$$\frac{\partial}{\partial t}(\rho v)+\frac{\partial}{\partial x}(\rho uv)+\frac{\partial}{\partial y}(\rho vv)+\frac{\partial}{\partial z}(\rho wv)=-\frac{\partial P}{\partial y}+(v+v_t)\left(\frac{\partial^2 v}{\partial x^2}+\frac{\partial^2 v}{\partial y^2}+\frac{\partial^2 v}{\partial z^2}\right) \quad (2)$$

The momentum equation along the Z-axis;

$$\frac{\partial}{\partial t}(\rho w)+\frac{\partial}{\partial x}(\rho uw)+\frac{\partial}{\partial y}(\rho vw)+\frac{\partial}{\partial z}(\rho ww)=-\frac{\partial P}{\partial y}+(v+v_t)\left(\frac{\partial^2 w}{\partial x^2}+\frac{\partial^2 w}{\partial y^2}+\frac{\partial^2 w}{\partial z^2}\right) \quad (3)$$

The continuity equation;

$$\frac{\partial}{\partial x}(\rho u)+\frac{\partial}{\partial y}(\rho v)+\frac{\partial}{\partial z}(\rho w)=0 \quad (4)$$

The energy equation;

$$\frac{\partial}{\partial t}(\rho u)+\frac{\partial}{\partial x}(\rho uu)+\frac{\partial}{\partial y}(\rho vu)+\frac{\partial}{\partial z}(\rho wu)=-\frac{\partial P}{\partial x}+\mu\left(\frac{\partial^2 u}{\partial x^2}+\frac{\partial^2 u}{\partial y^2}+\frac{\partial^2 u}{\partial z^2}\right) \quad (5)$$

In solar chimney power plants, heat transfer occurs through natural convection in the airflow beneath the collector. The dimensionless Rayleigh equation for this natural convection is defined as follows:

$$Ra=\frac{g\beta\Delta T{H_c}^3}{\alpha\upsilon} \quad (6)$$

In Equation 6, the collector height in solar chimney power plants is denoted as H_c, the thermal diffusion coefficient as α and the kinematic viscosity as υ. In this study, since the Ra number is

greater than 10^9, the system is considered turbulent (Zandian and Ashjaee, 2010) [29]. ANSYS Fluent software is commonly preferred in the CFD analyses of SCPPs and it has been observed that three different RNG k-ε turbulence models are used in this software. Some researchers have preferred the standard RNG k-ε turbulence model, which is economical, provides accurate results in most flows and is independent of flow regime and geometry (Bayareh, 2017) [30]. In some specialized CFD modeling studies, the Realizable RNG k-ε turbulence model has been preferred (Kalantar and Zare, 2011) [31]. RNG k-ε turbulence model equation;

$$\frac{\partial}{\partial t}(\rho k) + \frac{\partial}{\partial x_i}(\rho k u_i) = \frac{\partial}{\partial x_j}\left[\left(\mu + \frac{\mu_t}{\sigma_k}\right)\frac{\partial k}{\partial x_j}\right] + G_k + G_b + \rho\varepsilon - Y_M + S_k \tag{7}$$

$$\frac{\partial}{\partial t}(\rho\varepsilon) + \frac{\partial}{\partial x_i}(\rho\varepsilon u_i) = \frac{\partial}{\partial x_j}\left[\left(\mu + \frac{\mu_t}{\sigma_\varepsilon}\right)\frac{\partial \varepsilon}{\partial x_j}\right] + C_{1\varepsilon}\frac{\varepsilon}{k}(G_k + C_{3\varepsilon}G_b) - C_{2\varepsilon}\rho\frac{\varepsilon^2}{k} - R_e + S_\varepsilon \tag{8}$$

In this context, G_k denotes the production of turbulent kinetic energy from mean velocity gradients, while G_b denotes the production of turbulent kinetic energy from buoyancy forces. Additionally, Y_M represents the contribution of fluctuating dilatation in compressible turbulence to the total dissipation rate. Furthermore, S_ϵ and S_k are user-defined source terms depending on the specific study. Furthermore, α_k and α_ϵ represent the turbulent Prandtl numbers for turbulent kinetic energy and turbulent dissipation, respectively. The eddy viscosity μ_t is calculated (Shih et al., 1995);

$$\mu_t = \rho C_\mu \frac{k^2}{\varepsilon} \tag{9}$$

The value of C_μ is calculated from Equation 10 (Shih et al., 1995);

$$C_\mu = \frac{1}{A_0 + A_s\frac{kU^*}{\varepsilon}} \tag{10}$$

$$U^* = \sqrt{S_{ij}S_{ij} + \tilde{\Omega}_{ij}\tilde{\Omega}_{ij}} \tag{11}$$

$$\tilde{\Omega}_{ij} = \bar{\Omega}_{ij} - \varepsilon_{ijk}\omega_k - 2\varepsilon_{ijk}\omega_k \quad (12)$$

In solar chimney power plants, there are different approaches to calculating the density of air as its temperature rises along the collector. In this study, the Boussinesq model, which has been validated by previous studies to give the best results for limited temperature increases in the Manzanares prototype, is used (Bayareh, 2017) [30]. In this approach, the density calculation is performed using the following equation:

$$(\rho - \rho a)g \approx -\rho a\beta(T - Ta)g \quad (13)$$

In the related equation, β represents the thermal expansion coefficient, $\rho\alpha$ represents the density of the inlet air of the system and $T\alpha$ represents its temperature. As previously mentioned, thermal energy input in solar chimney power plants occurs through the collector section with semi-transparent properties.

The total energy ($\dot{Q}$) can be computed with the following equation:

$$\dot{Q} = \dot{m}C_p\Delta T \quad (14)$$

$$\Delta T = T_{out} - T_{in} \quad (15)$$

In the equation, ΔT denotes the temperature difference between the air's inlet and outlet along the collector. The collector is exposed to direct solar radiation flux. In this case, for the collector area A_{coll} and the radiation flux G, the efficiency of the collector can be calculated using the following equation:

$$\eta_{coll} = \frac{\dot{Q}}{A_{coll}G} \quad (16)$$

Several methods for determining the output power of SCPPs are available in the literature. A frequently employed method is to determine the output power by assessing the pressure drop across the turbine (Kalantar and Zare, 2011) [31]. This method can be expressed as follows:

$$P_0 = \eta_t \Delta p_t Q_v \tag{17}$$

In the related equation, η_t represents the turbine-generator efficiency, which is generally accepted as 0.8 in the literature. Δp_t denotes the turbine pressure drop and Q_v represents the volumetric flow rate. Despite various approaches found in the archieve, in this work, the turbine pressure drop (Δp_t) is calculated using the average pressure at the location where the turbine is positioned (ΔP_t), as demonstrated in the following equation:

$$\Delta P_t = r_t P_t \tag{18}$$

In this equation, r_t represents the turbine pressure drop ratio, which is generally accepted as 2/3 in the literature (Li et al., 2016) [32]. Another commonly used performance criterion in the performance analysis of solar chimney power plants is system efficiency. The efficiency of the system is calculated using the following equation:

$$\eta = \frac{P_0}{A_{coll} G} \tag{19}$$

3. SYSTEM ANALYSIS AND CFD MODEL

When designing an SCPP, a multitude of variables must be taken into account. In this work, numerical analyses were performed using a three-dimensional axisymmetric CFD model, referencing the world's first application, the Manzanares prototype in Spain. The data for this prototype are shown in Table 1.

Table 1. Geometric dimensions of the Manzanares Solar Chimney Power Plant

Geometric Parameter	**Value**
Chimney Height (L)	194.6 m

Collector Height (L_c)	1.85 m
Chimney Radius (D/2)	5.0 m
Collector Radius (D_s/2)	122.0 m
Ground Thickness	0.5 m

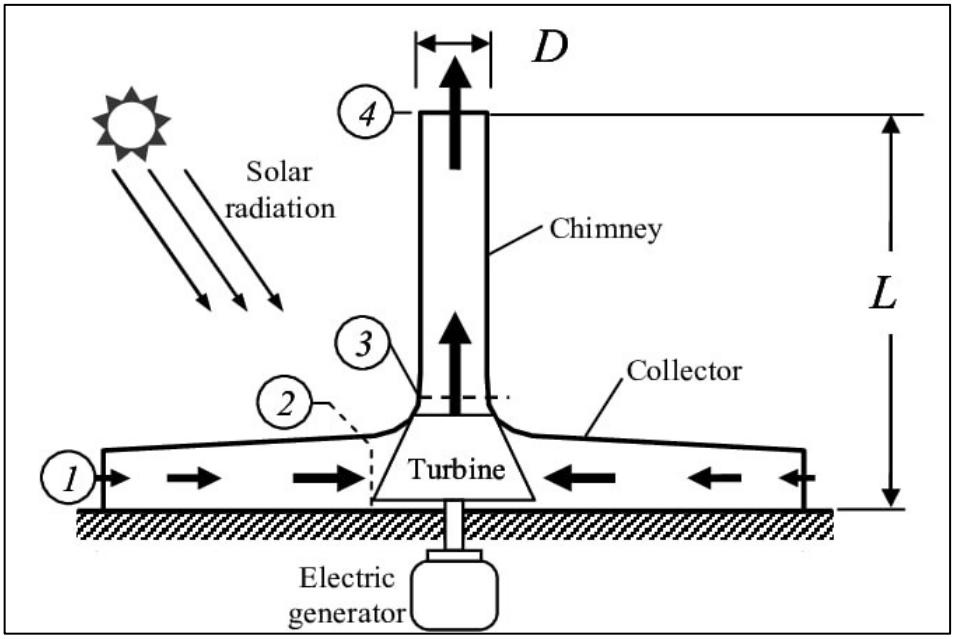

Figure 2. Schematic diagram of SCPP

In this article, the impacts of collector height, chimney height and chimney radius on the system will be analyzed. The parameters to be adjusted in this context are detailed in Table 2.

Table 2. Variable parameters to be examined in the analysis

Geometric Parameter	Value
Collector Height (Lc)	1.5-2.5
Chimney Radius (D/2)	4-5.5
Chimney Height (L)	50-250

The design parameters with the value ranges given above have been systematically implemented using the Central Composite experimental design method. In this design, where a total of 15 analyses were conducted, the first 5 parameters examine the effect of chimney height, the next 5 parameters examine the effect of chimney radius and the last 5 parameters examine the effect of

collector height on the system. All analyses were repeated using both the RNG k-ε and SST k-ω turbulence models separately, allowing for an investigation of the impact of these two different turbulence models on the results.

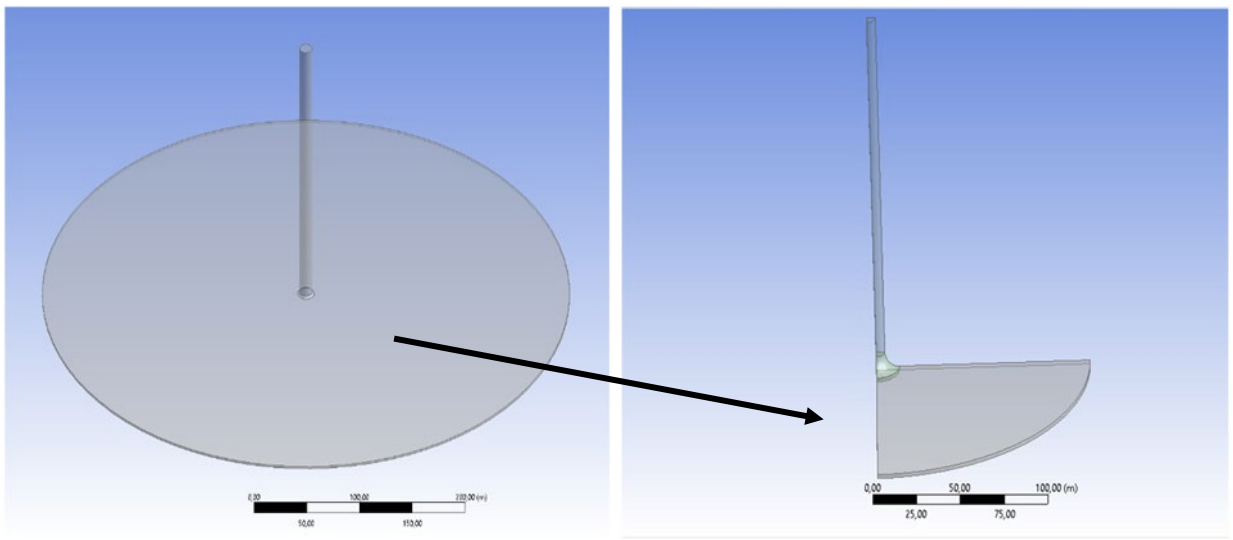

Figure 3. SCPP model and 90° symmetric cross-section view

Experimental data from prior studies suggest that the temperature remains unchanged below a depth of 0.5 meters from the ground level over time [17]. Therefore, the ground thickness has been set to 0.5 m in this study (Haaf, 1984). The CFD model was developed using ANSYS Fluent. Due to the study's scope, the developed three-dimensional CFD approach requires a dense mesh for numerical modeling and the iteration time for each parametric study can take several hours. To ensure economic efficiency, a 90° symmetric model was created instead of modeling the entire geometry. Accurate identification of the physical properties of the chimney, collector and ground materials is vital for the numerical modeling of solar chimney power plants. The material parameters used in the study are detailed in Table 3.

Table 3. Physical properties of materials used in the CFD Model

Physical Property (Unit)	**Collector Surface (Glass)**	**Chimney (Aluminum)**	**Ground (Gravel/Sand)**
Density (Kg/m^3)	2500	2719	2160
Specific Heat Capacity (J/kgK)	750	871	710
Thermal Conductivity (W/mK)	1.15	202.4	1.83

Emissivity	0.1	1	0.9
Transmittance	0.9	Opaque	Opaque
Thickness (m)	0.004	0.00125	0.5
Refractive Index	1.526	1	1

Similarly, the climatic parameters and the properties of the air used are detailed in Table 4:

Table 4. Environmental parameters and thermophysical properties of the model

Physical Property (Unit)	**Value**
Ambient Temperature (K)	293.15
Ambient Pressure (Pa)	101325
Ambient Air Density (kg/m³)	1.2046
Thermal Conductivity of Air (W/mK)	0.0259
Specific Heat Capacity of Air (J/kgK)	1006.43

The properties listed in Table 3 and Table 4 remained constant for the duration of the study. It was assumed that the pressure at the chimney inlet remained unchanged and outlet and that the temperature at the collector inlet was equal to the ambient air temperature. Based on the adiabatic boundary condition on the ground and chimney wall, the heat transfer coefficient was assumed to be h=0 W/m²K for the ground and h=10 W/m²K between the collector and system air.

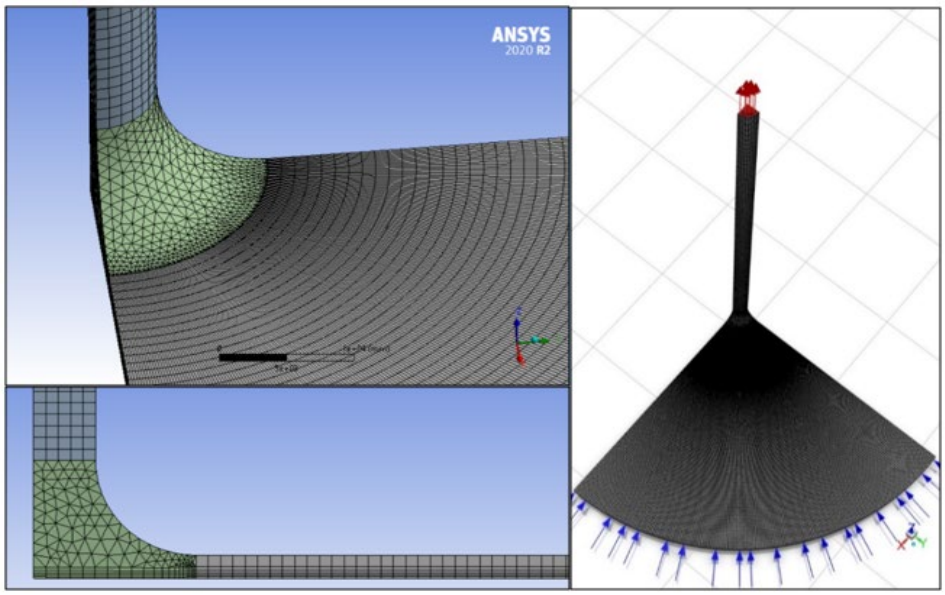

Figure 4 : Model meshing and determination of pressure inlet and outlet

After defining the design parameters of the SCPP in the numerical analysis program, the system must be divided into numerous small segments for analysis. These segments are referred to as 'mesh'. Increasing the number of mesh elements divides the system into finer parts, leading to more precise results in numerical analysis. Figure 4 illustrates the mesh structure of the solar chimney. The model in Figure 4 is an SCPP model with a chimney height of 200 meters. Considering these features, a mesh element count of 158114 and a node count of 164090 were obtained for the 200 meter chimney height. Obtaining accurate data in the analysis is directly related to the mesh structure and its properties. Therefore, the meshing process should be performed carefully and accurately. Analyses should be carried out considering mesh quality. Once the mesh structure was completed, the problem was defined in the numerical analysis software. The inlet pressure to the collector and the outlet pressure from the chimney were assumed to be p_{in}=0 Pa and p_{air}=101325 Pa, respectively, compared to the atmospheric pressure. Additionally, the boundary condition of the chimney wall was also adiabatic. The boundary conditions are detailed in Table 5.

Table 5. Boundary conditions

Boundary	**Type**	**Conditions**
Collector Inlet (inlet)	Pressure inlet	p_{in} = 0 Pa, T_{air} = 293.15 K, h = 10 W/m^2
Collector Surface(ch surf.)	Transparent	T_0 = 293.15 K (20°C), Rad. = 1000W/m^2
Ground (ground)	Opaque / Adiabatic	T = 293.15 K (20°C)
Chimney Outlet (outlet)	Pressure outlet	p_{out}=p_{in}−ρ.g.H
Chimney(chimney)	Opaque / Adiabatic	q_{ch} = 0 W/m^2

The conservation equations were discretized using the finite volume method and simulations were conducted using the ANSYS Fluent program. The momentum equations were solved using the RNG k-ε and SST k-ω turbulence models and the relationship between air velocity and pressure was determined using the SIMPLE algorithm. The PRESTO approach was preferred for pressure interpolation. The conservation equations were discretized through the use of the second-order UPWIND method. The DO (Discrete Ordinates) radiation model was utilized to track solar radiation in the simulations. For this purpose, the Solar Ray Tracing model was chosen from the Radiation model. The Fair Weather Conditions method was selected for Solar irradiation and using the solar calculator interface, the sun direction vector was determined as -0.295, 0.925, -0.237

unit direction vectors. The Boussinesq method was chosen to calculate changes in air density. The convergence criterion was set to 10^{-6} .

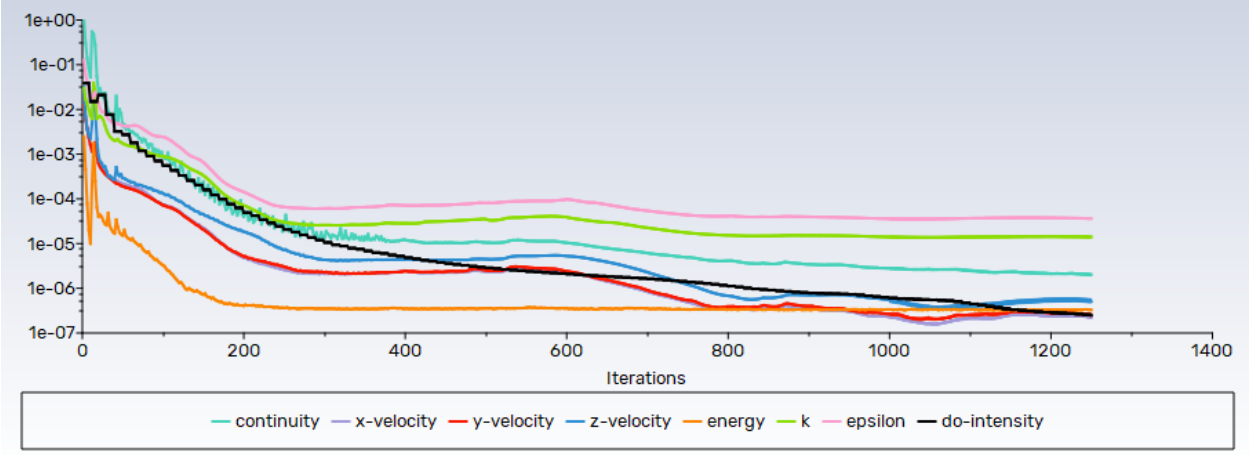

Figure 5 : Residual stress graphs

In the study, both the RNG k-ε and SST k-ω turbulence models have been used to analyze the performance of the Solar Chimney Power Plant (SCPP). These models are widely used in CFD simulations to predict turbulent flow behavior, each with distinct advantages and limitations. The comparison of results from these models is essential to understand their impact on the system's performance. RNG k-ε turbulence model solves two transport equations for the turbulent kinetic energy (k) and its dissipation rate (epsilon). It is computationally efficient and provides reliable results for free-shear flows, such as jets and mixing layers and the model is less accurate in near-wall regions and for flows with strong adverse pressure gradients or separation. SST k-ω turbulence model solves for the turbulent kinetic energy (k) and the specific dissipation rate (omega), offering improved near-wall treatment. The model excels in predicting flows with adverse pressure gradients and boundary layer separations and it can be more sensitive to inlet conditions and is computationally more expensive.

4. RESULTS AND DISCUSSION

In this study, the numerical analysis results obtained using ANSYS Fluent software were validated by comparing them with the data obtained for the Manzanares prototype by Haaf (1984) in the literature. According to the experimental data from the Manzanares prototype, the outlet velocity is 15 m/s. In this study, the values obtained are 14.173 m/s for the RNG k-ε turbulence model and 13.56 m/s for the SST k-ω turbulence model. The outlet temperature for the experimental prototype

is 313 K, while the values obtained in this study are 309.62 K for the RNG k-ε turbulence model and 308.33 K for the SST k-ω turbulence model.

In the SCPP system, 15 different numerical analyses were conducted using the Central Composite experimental design table for the selected parameters of chimney height, chimney radius and collector height. As a result of the analyses, Figure 6 shows the velocity gradients with a chimney height of 200 meters, a chimney diameter of 5 meters and a collector height of 1.85 meters.

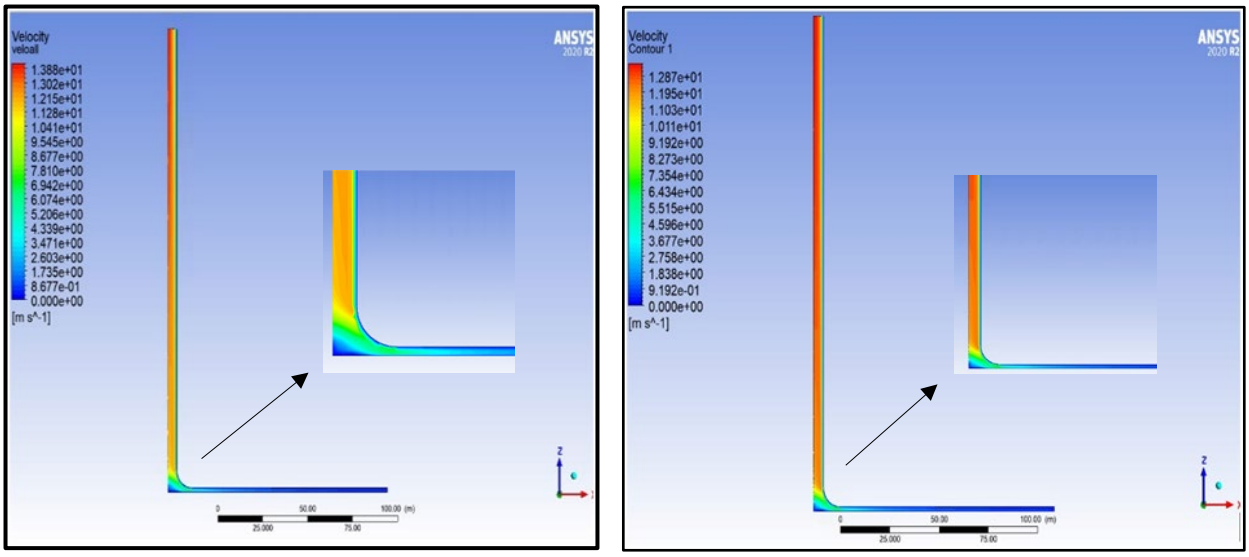

Figure 6. a) RNG k-ε velocity gradient b) SST k-ω velocity gradient

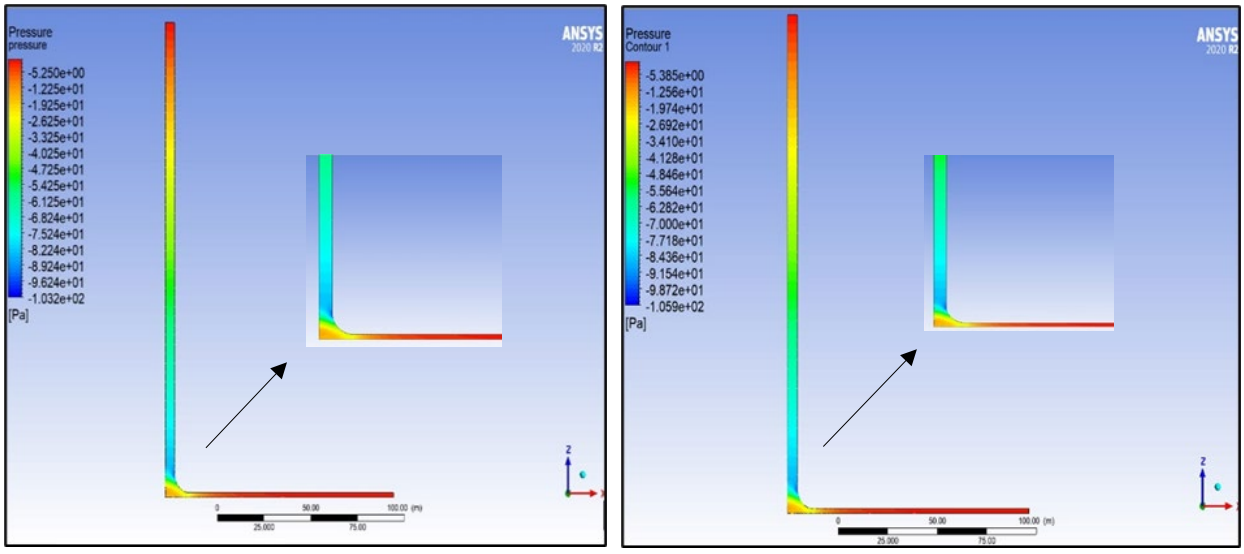

Figure 7. a) RNG k-ε pressure gradient b) SST k-ω pressure gradient

As shown in Figure 6, the velocity reaches its maximum in the narrow section of the chimney. In the collector section, the velocity is very low due to natural convection. Therefore, the lowest velocity is in the collector section. However, the heated air reaching the chimney will rise and its velocity will increase. This is clearly demonstrated in the figures above. Likewise, Figure 7 shows the pressure gradients formed in the SCPP with the same parameters.

In many studies, it is assumed that the pressures at the inlet and outlet are equal, so pressure gradients are measured at ground level with atmospheric pressure at the chimney outlet and some negative pressures occur at the chimney inlet. In Figure 7, it is evident that the pressure decreases steadily from ground level to the chimney outlet. The temperature gradient formed at the inlet section of the 200 meter high chimney is also shown in detail in Figure 8.

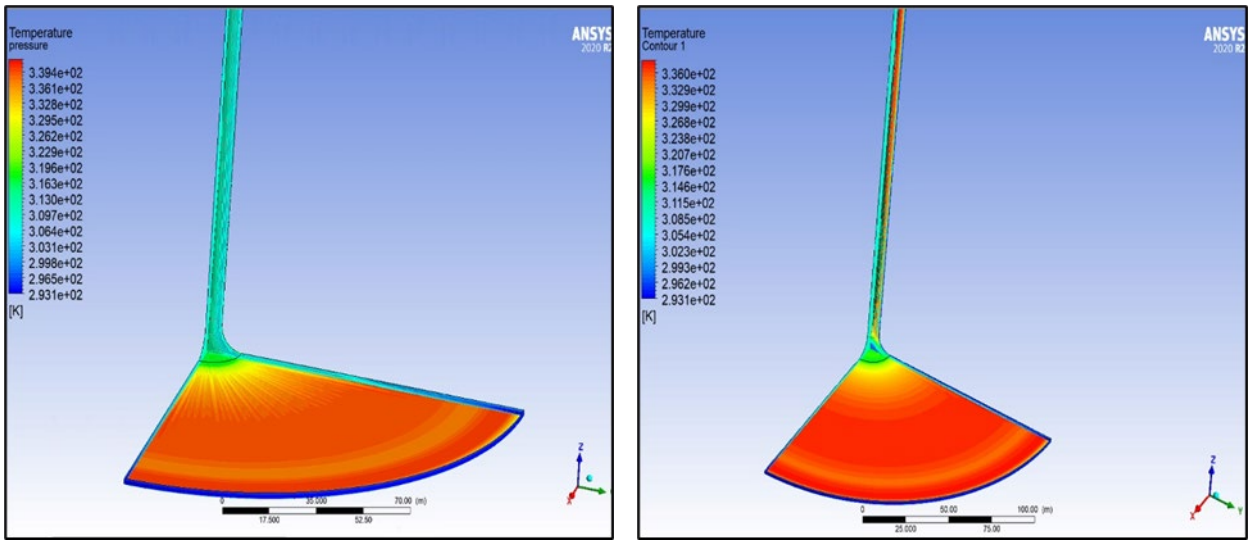

Figure 8. a) RNG k-ε temperature gradient b) SST k-ω temperature gradient

When the ground absorbs solar radiation, the surface temperature rises. This growing temperature difference between the air and the ground enhances the heat transfer rate, causing the air temperature close to the ground to increase.

For Figure 9 and 10, the chimney radius was kept constant at 5 meters and the collector height was kept constant at 1.85 meters. As the air moves towards the center of the collector, its temperature rises until it reaches the chimney entrance. At the area just below the chimney entrance, the temperature hits its peak. Subsequently, as the air ascends through the chimney, the temperature becomes evenly distributed and the average temperature stays constant within the thermally

insulated chimney. Analyses were conducted using five different chimney heights. The results of these analyses, showing the velocity and temperature values at the chimney outlet, are presented in the graphs (Figure 9-10).

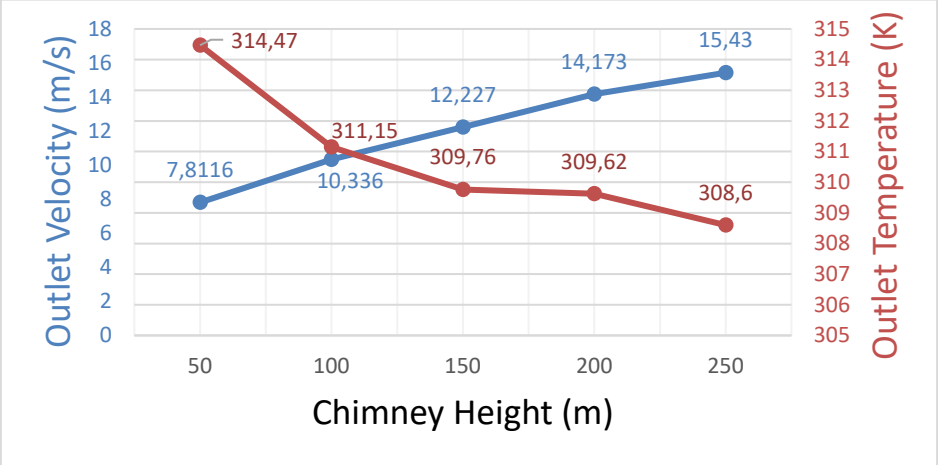

Figure 9. Effect of chimney height on outlet temperature and velocity in the RNG k-ε model

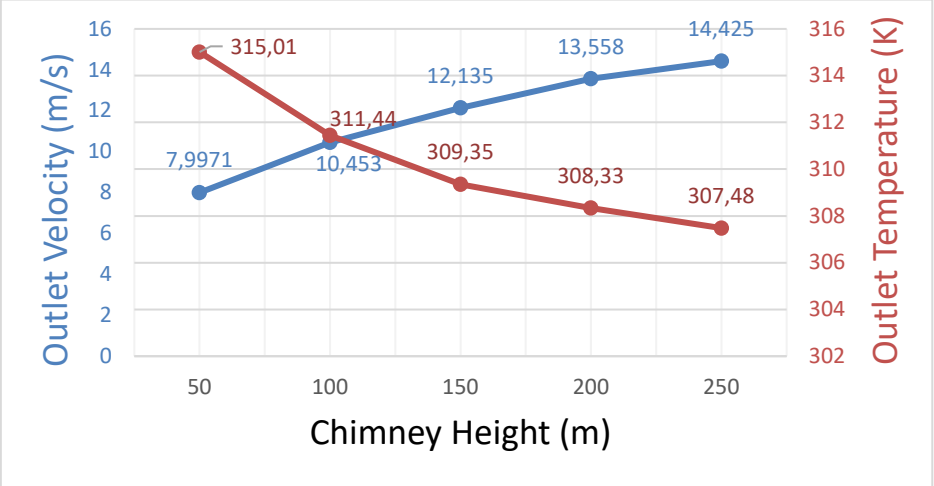

Figure 10. Effect of chimney height on outlet temperature and velocity in the SST k-ω model

Upon examining the above graphs, the effect of chimney height on the system can be observed. According to Figure 9, an increase in chimney height results in a linearly proportional increase in outlet velocity. In contrast, outlet temperature shows an inversely proportional decrease with chimney height. This decrease is sharp in the 50-100 m range, while it is less pronounced in the 150-200 m range. For Figure 10, the SST k-ω turbulence model used in the analysis exhibits different behavior in outlet temperature compared to the RNG k-ε turbulence model within the

150-200 m range. Accordingly, while no significant decrease is observed in Figure 9, a notable decrease continues in Figure 10.

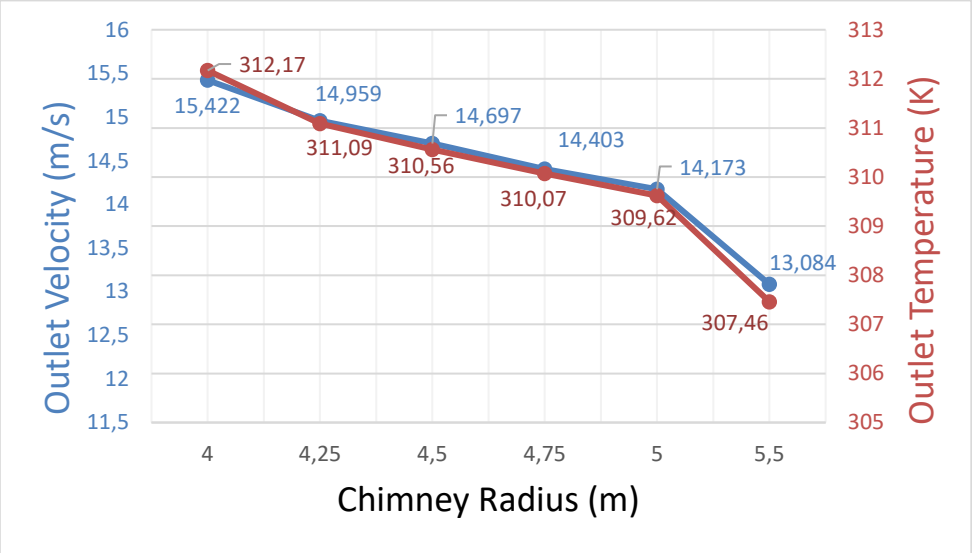

Figure 11. Effect of chimney radius on outlet temperature and velocity in the RNG k-ε model

For Figure 11 and 12, the chimney height was kept constant at 200 meters and the collector height at 1.85 meters. According to Figure 11, as the chimney radius increases, both the outlet velocity and temperature values exhibit similar behavior by decreasing and this decrease becomes pronounced when the chimney radius reaches 5 meters. The maximum outlet velocity and temperatures were observed for the minimum chimney radius of 4 meters. The minimum values occurred at the maximum chimney radius.

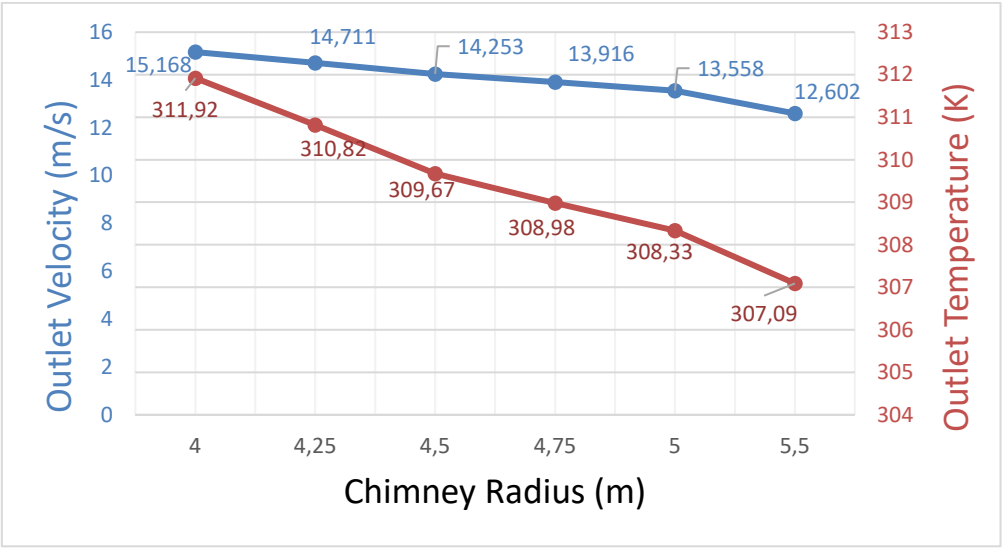

Figure 12. Effect of chimney radius on outlet temperature and velocity in the SST k-ω model

Upon examining Figure 12, It is apparent that as the chimney radius enlarges, both velocity and temperature values decline. This rate of decrease is more pronounced for temperature compared to velocity. In this context, increasing the chimney radius will negatively impact the system both in terms of cost and efficiency.

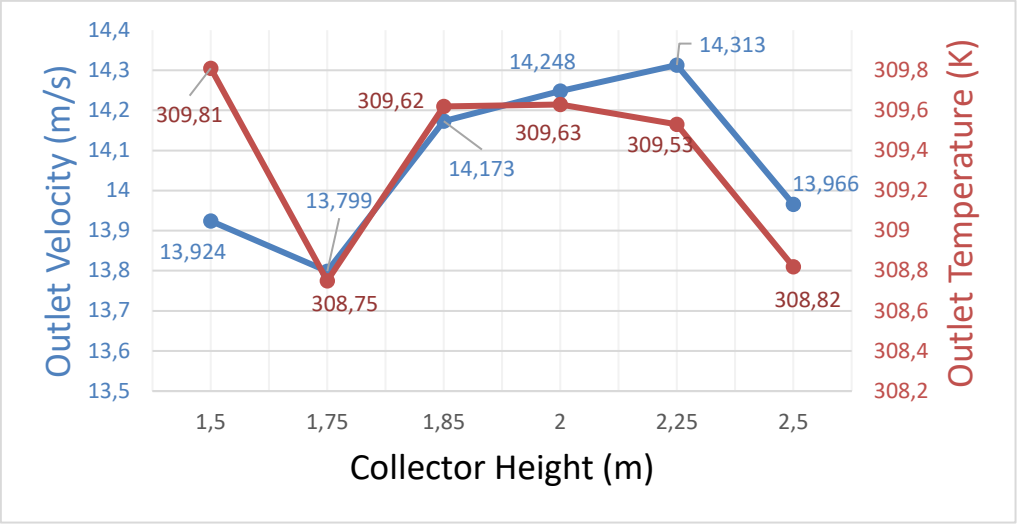

Figure 13. Effect of collector height on outlet temperature and velocity in the RNG k-ε model

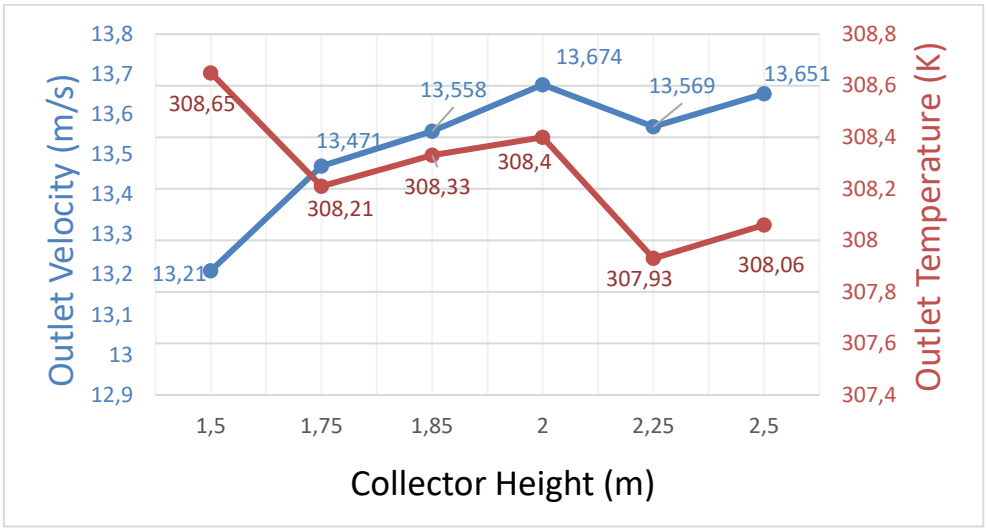

Figure 14. Effect of collector height on outlet temperature and velocity in the SST k-ω model

For Figure 13 and 14, with a chimney height of 200 m and a radius of 5 meters kept constant, the influence of collector height on the system is observed. In the range of 1.50 m to 1.75 m collector height, there is a decreasing trend in velocity for the RNG k-ε turbulence model, while an increasing trend is observed for the SST k-ω turbulence model. Between 1.75 m and 1.85 m, both

turbulence models show similar increases in velocity and pressure values. From 1.85 m to 2 m, velocity increases in both models, but there are some differences in temperature behavior between them. From 2 m to 2.25 m, both models exhibit a decreasing trend in temperature, while velocity increases for the RNG k-ε model and decreases for the SST k-ω model. Examining further points, between 2.25 m and 2.5 m, velocity and temperature decrease in the RNG k-ε turbulence model, whereas they show a linear increase in the SST k-ω model. These findings underscore the importance of considering different turbulence models in conducting analyses.

As a result, the analysis examined the effects of chimney height, chimney diameter and collector height on the system across 30 different parameters using two different turbulence models.

5. CONCLUSION

This study conducted a comprehensive investigation into the effects of various design parameters on the performance of Solar Chimney Power Plants (SCPP) using two different turbulence models (RNG k-ε and SST k-ω). The findings highlight several important insights for optimizing system performance;

- The height of the chimney significantly affects the outlet velocity and temperature. An increase in chimney height leads to a notable rise in outlet velocity, which enhances the power generation capacity of the SCPP. However, it also results in a decrease in outlet temperature. For instance, increasing the chimney height from 100 meters to 200 meters increased the outlet velocity by 35% and decreased the outlet temperature by 20%. This indicates the need to balance speed and thermal performance.
- The radius of the chimney is inversely related to both outlet velocity and temperature. Larger chimney radius reduce the velocity and temperature at the outlet, which can negatively impact system efficiency. For optimal performance, the design must balance these effects. For example, increasing the chimney radius from 4 meters to 5.5 meters resulted in a 15% decrease in outlet velocity and a 10% decrease in outlet temperature.
- Changes in collector height exhibit complex behaviors in both turbulence models. The RNG k-ε model shows more sensitivity with rapid changes in outlet velocity and temperature, while the SST k-ω model demonstrates more stable transitions. For example, increasing the collector height from 1.5 meters to 2.5 meters led to a 20% increase in outlet velocity in the RNG k-ε model but only a 10% increase in the SST k-ω model. Additionally, higher collector heights

allowed the air to warm up longer, resulting in higher temperature increases, though this may affect the overall structural stability of the system.

- The RNG k-ε model responds more quickly and sensitively to design changes, making it suitable for detailed performance tuning, whereas the SST k-ω model offers more stable and predictable behavior, which can be advantageous for overall system stability and long-term operation. The RNG k-ε model can rapidly adjust outlet velocity and temperature in response to changes in chimney height, while the SST k-ω model maintains system stability with smoother transitions. This is particularly beneficial for reducing long-term operation and maintenance costs.

In conclusion, the choice of design parameters and turbulence models plays a critical role in optimizing the performance of Solar Chimney Power Plants. Future research should focus on exploring additional geometric and operational parameters and integrating experimental data to further validate and enhance the numerical models used in this study. Additionally, further studies on how different turbulence models perform under various operational scenarios will be valuable. The insights gained from this research can contribute to the development of more efficient and cost-effective SCPPs, promoting the use of renewable energy sources. In conclusion, the study makes significant contributions to the literature by comparing the effects of different turbulence models on the thermal and fluid dynamic characteristics of Solar Chimney Power Plants (SCPP). This allows for the development of more precise and reliable models for the design and optimization of SCPPs.

NOMENCLATURE

SCPP: Solar Chimney Power Plant
RNG k-ε: K-epsilon turbulence model
SST k-ω: K-omega turbulence model

DECLARATION OF ETHICAL STANDARDS

The authors of the paper submitted declare that nothing which is necessary for achieving the paper requires ethical committee and/or legal-special permissions.

CONTRIBUTION OF THE AUTHORS

Fuat Tan: Analysis, investigation, writing, methodology,

Alp Eren Dede: Recources, writing, methodology

CONFLICT OF INTEREST

There is no conflict of interest in this study.

REFERENCES

[1] Tawalbeh M, Al-Othman A, Singh K, Douba I, Kabakebji D, Alkasrawi M. Microbial desalination cells for water purification and power generation: a critical review. Energy 2020; 209: 118493.

[2] Kumari U, Swamy K, Gupta A, Karri RR, Meikap BC. Global water challenge and future perspective. Green Technologies for the Defluoridation of Water. Elsevier 2021; 197–212.

[3] Kalogirou SA. Seawater desalination using renewable energy sources. Prog. Energy Combust. Sci 2005; 31: 242–281.

[4] IEA. World energy outlook. 2018.

[5] Wang W, Fan LW, Zhou P. Evolution of global fossil fuel trade dependencies. Energy 2022; 238: 121924.

[6] Tawalbeh M, Javed MN, Al-Othman A, Almomani F. The novel advancements of nanomaterials in biofuel cells with a focus on electrodes' applications. Fuel 2022; 322: 124237.

[7] San Cristobal J. Multi-criteria decision-making in the selection of a renewable energy project in Spain: the Vikor method. Renew. Energy 2011; 36(2): 498-502.

[8] Maghrabie HM, Abdelkareem MA, Elsaid K, Sayed ET. A review of solar chimney for natural ventilation of residential and non-residential buildings. Sustain. Energy Technol. Assessments 2022; 52: 102082.

[9] Trieb F, Langniß O, Klaiß H. Solar electricity generation - a comparative view of technologies, costs and environmental impact. Sol. Energy 1997; 59: 89-99.

[10] Kiwan S, Al-Nimr M, Salim I. A hybrid solar chimney/photovoltaic thermal system for direct electric power production and water distillation. Sustain. Energy Technol. Assessments 2020; 38: 100680.

[11] Tawalbeh M, Mohammed S, Alnaqbi A, Alshehhi S, Al-Othman A. Analysis for hybrid photovoltaic/solar chimney seawater desalination plant: A CFD simulation in Sharjah, United Arab Emirates. Renewable Energy 2023; 202: 667-685.

[12] Haaf W. Solar chimneys. Part II: preliminary test results from the Manzanares pilot plant. Solar Energy 1984; 2: 141-161.

[13] Nizetic S, Ninic N, Klarin B. Analysis and feasibility of implementing solar chimney power plants in the Mediterranean region. Energy 2008; 33: 1680-1690.

[14] Zhou X, Yang J, Xiao B, Hou G, Xing F. Analysis of chimney height for solar chimney power plant. Applied Thermal Engineering 2009; 29: 178-185.

[15] Fluri TP, Backstrom TWV. Performance analysis of the power conversion unit of a solar chimney power plant. Solar Energy 2008; 82: 999-1008.

[16] Larbi S, Bouhdjar A, Chergui T. Performance analysis of a solar chimney power plant in the southwestern region of Algeria. Renewable and Sustainable Energy Reviews 2010; 14(1): 470-477.

[17] Maia CB, Ferreira AG, Valle RM, Cortez MFB. Theoretical evaluation of the influence of geometric parameters and materials on the behavior of the airflow in a solar chimney. Computers & Fluids 2009; 38: 625-636.

[18] Khelifi C, Ferroudji F, Ouali M. Analytical modeling and optimization of a solar chimney power plant. International Journal of Engineering Research in Africa 2016; 25: 78-88.

[19] Cüce E. Güneş Bacası Güç Santrallerinde Toplayıcı Eğiminin Çıkış Gücüne ve Sistem Verimine Etkisi. Uludağ Üniversitesi Mühendislik Fakültesi Dergisi 2020; 25(2).

[20] Cuce PM, Cuce E, Mandal DK, Gayen DK et.al. ANN and CFD driven research on main performance characteristics of solar chimney power plants: Impact of chimney and collector angle. Case Studies in Thermal Engineering 2024; 60: 104568.

[21] Mandal DK, Biswas N, Manna N, Benim AC. Impact of chimney divergence and sloped absorber on energy efficacy of a solar chimney power plant (SCPP). Ain Shams Engineering Journal 2024; 15(2).

[22] Biswas N, Mandal D, Bose S, Manna N, Benim A.C. Experimental Treatment of Solar Chimney Power Plant-A Comprehensive Review. Energies 2023; 16(17): 6134.

[23] Biswas N, Mandal D, Manna N, Benim AC. Novel stair-shaped ground absorber for performance enhancement of solar chimney power plant. Applied Thermal Engineering 2023; 227: 120466.

[24] Mandal D, Biswas N, Barman A, Chakraborty R, Manna N. A novel design of absorber surface of solar chimney power plant (SCPP): Thermal assessment, exergy and regression analysis. Sustainable Energy Technologies and Assessments 2023; 56: 103039.

[25] Mandal D, Biswas N, Manna N, Gayen D, Benim AC. An application of artificial neural network (ANN) for comparative performance assessment of solar chimney (SC) plant for green energy production. Scientific Reports 2024; 979.

[26] Navarro J.M.A, Ruiz V.A, Hinojosa J.F, Moreno S, Maytorena V.M. Transient Thermal Analysis of a Double Duct Solar Roof Chimney Coupled With a Scaled Room. Journal of Solar Energy Engineering 2024; 146(1): 011008.

[27] Maia C.B, Silva J.O.C. CFD Analysis of a Small-Scale Solar Chimney Exposed to Ambient Crosswind. Sustainability 2022; 14(22): 15208.

[28] Önal M, Koç A, Köse Ö, Koç Y, Yağlı H. Numerical Examination of a Solar Chimney Power Plant Designed for the Iskenderun Region. Konya Mühendislik Bilimleri Dergisi 2022; 10(3): 548-562.

[29] Ashjaee M, Zandian A, The thermal efficiency improvement of a steam Rankine cycle by innovative design of a hybrid cooling tower and a solar chimney concept. Renewable Energy 2010; 51: 465-473.

[30] Bayareh M. Numerical simulation of a solar chimney power plant in the southern region of Iran. Energy Equipment and Systems 2017; 5(4): 431-437.

[31] Kalantar V, Zare M. Simulation of flow and heat transfer in 3D solar chimney power plants-numerical analysis. Jordan International Energy Conference 2011.

[32] Li J, Guo H, Huang S. Power generation quality analysis and geometric optimization for solar chimney power plants. Solar Energy 2016; 139: 228-237.